Enhanced activity of carbon-supported Pd–Pt catalysts in the hydrodechlorination of dichloromethane

M. Martin-Martinez [*], L.M. Gómez-Sainero, J. Bedia, A. Arevalo-Bastante, J.J. Rodriguez

Sección Departamental de Ingeniería Química, Facultad de Ciencias, Universidad Autónoma de Madrid, Cantoblanco, 28049 Madrid, Spain

ARTICLE INFO

ABSTRACT

Monometallic and bimetallic catalysts with different proportions of Pd and Pt prepared by co-impregnation on activated carbon have been deeply characterized by inductively coupled plasma-mass spectroscopy, temperature-programmed reduction, 77 K N_2 adsorption–desorption, CO chemisorption, transmission electron microscopy, X-ray diffraction and X-ray photoelectron spectroscopy. They have been tested in the gas-phase hydrodechlorination of dichloromethane (DCM) at atmospheric pressure, reaction temperatures of 150–200 °C, and a space-time of 0.6 kg h mol^{-1}. The presence of Pd and Pt in the catalysts produces a synergistic effect observed in terms of dichloromethane conversion and overall dechlorination, especially when both metals are in similar proportions. The results from catalysts characterization suggest that the enhanced activity is due to a significant decrease of the metallic particles size and an optimum ratio of electro-deficient to zero-valent species in the bimetallic catalysts. The catalyst with 0.90 wt.% of Pt and 0.50 wt.% of Pd yielded the best results. Under intensified conditions, viz. 250 °C and 1.73 kg h mol^{-1}, 100% DCM conversion and 98.6% overall dechlorination were obtained. This catalyst had most of its metallic particles within the range of 0.5–1 nm.

© 2015 Elsevier B.V. All rights reserved.

1. Introduction

Air pollution has become a problem of growing interest and consequently stringent regulations have been developed for the emission of pollutants to the atmosphere. Dichloromethane (DCM) is a chlorinated volatile organic compound with high environmental impact, due to its toxicity and carcinogenic character and its contribution to the depletion of the ozone layer, the global warming and the formation of photochemical smog [1–4]. Despite these harmful effects, its use in chemical and pharmaceutical industry is still widely extended (e.g., in paint strippers, in the manufacture of film coatings, in metal cleaning and finishing processes for the electronics industry, as a blowing agent in the manufacture of polyurethane foams, in bitumen testing, in the preparation of drugs, pharmaceuticals, decaffeinated teas and coffees, and hops for the brewing industry or as a post-harvest fumigant for grains and fruits) [5]. Its particular physical and chemical properties (high stability, low flammability, high volatility and high solvent capacity) make difficult its substitution in a number of processes. Hence,

the development of suitable technologies for the removal of this toxic and similar contaminants in off-gas streams is necessary. Among these technologies catalytic hydrodechlorination (HDC) has a promising potential since it can operate under relatively mild conditions, transforming the organochlorinated compounds like DCM into less toxic products and it is effective within a wide range of pollutant concentrations allowing to control the reaction products [6–8]. Recently it has been also explored by our research group as an alternative technology for the production of valuable hydrocarbons with promising results [9]. On the opposite, thermal treatments-like incineration and catalytic combustion, which are the main current technologies for the removal of these pollutants, may lead to strongly hazardous byproducts such us dioxins, chloro-furans and phosgene [10–12].

The literature on HDC shows a growing number of studies where a wide diversity of catalysts are employed. The most commonly used are those based on noble metals [13–15] and among them, Pd and Pt catalysts have demonstrated high HDC activity, being highly selective to non-chlorinated products, specially the Pd ones due to the capacity of this metal to dissociate de H_2 molecule, favouring the C–Cl hydrogenolysis [16–18]. In order to improve the efficiency and/or minimize the cost, those metals are commonly supported on a porous material. The interaction between the active phase and the support may affect the reaction by increasing the surface area,

* Corresponding author at: Ingeniería Química, Facultad de Ciencias, Universidad Autónoma de Madrid, Campus de Cantoblanco, Ctra. Colmenar Km 15, 28049 Madrid, Spain. Fax: +34 91 497 3516.
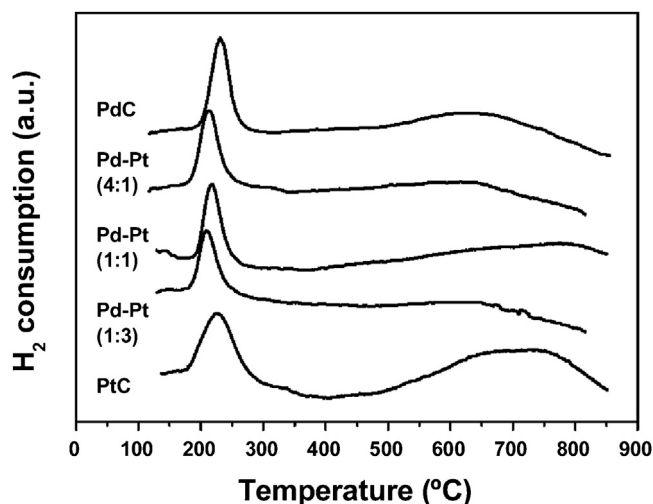*E-mail address:* maria.martin.martinez@uam.es (M. Martin-Martinez).

Fig. 1. TPR profiles of the catalysts.

Table 1
Catalysts prepared.

Notation	Nominal wt.%		μmoles per gram	
	Pd	Pt	Pd	Pt
PtC	0	1.80	0	96
Pd–Pt (1:3)	0.25	1.34	24	72
Pd–Pt (1:1)	0.50	0.90	48	48
Pd–Pt (4:1)	0.80	0.36	77	19
PdC	1.00	0	96	0

$\approx$750 m^2 g^{-1}; $V_{micro} \approx$0.30 cc g^{-1}; bulk density $\approx$0.5 g cm^{-3}; particle size: 0.25–0.50 mm) were prepared by co-impregnation, using aqueous solutions of PdCl$_2$ and/or H$_2$PtCl$_6$ (Sigma–Aldrich) of the required concentrations to get catalysts with 0 to 1 wt.% Pd loading, balanced with Pt to obtain the same overall atomic concentration of active phase in all of them (86 μmol/g). The catalysts were dried overnight at room temperature and heated under air atmosphere to 100 °C at 20 °C h^{-1}, the final temperature being maintained for 2 h. Their activation was carried out by heating them up to 250 °C (at 10 °C min^{-1}) under a continuous H$_2$ flow (50 Ncm^3 min^{-1}, supplied by Praxair, with a minimum purity of 99.999%) and maintaining these conditions for 2 h. The notation (describing the Pd/Pt atomic ratio) and the nominal active phase concentration of the catalysts prepared are summarized in Table 1.

2.2. Catalysts characterization

Bulk metal content was determined using inductively coupled plasma-mass spectroscopy (ICP-MS Elan 6000, Perkin-Elmer Sciex). The samples were previously digested in a strongly acidic mixture (HNO$_3$:3HCl) and treated in a microwave oven (Milestone ETHOS PLUS).

Temperature-programmed reduction (TPR) was performed to analyze the reducibility of the metallic phase, using a Pulse-ChemiSorb 2705 Micromeritics apparatus equipped with a thermal conductivity detector (TCD). The samples were heated up to 800 °C at 5 °C min^{-1} in a continuous 5% H$_2$/Ar (30 Ncm^3 min^{-1}) stream.

To characterize the porous structure of the catalysts, 77 K N$_2$ adsorption–desorption isotherms were obtained (TriStar II 3020, Micromeritics). The samples were previously outgassed for 12 h at 150 °C and a residual pressure of 10^{-3} Torr (VacPrep 061, Micromeritics). The surface area (S_{BET}) was calculated by the BET equation and the micropore volume (V_{micro}) was obtained using the t-method [42–44].

Metal dispersion on the catalysts surface was determined by CO chemisorption at room temperature (PulseChemiSorb 2705, Micromeritics). The samples were previously reduced at 250 °C for 2 h under a continuous H$_2$ flow of 20 Ncm^3 min^{-1}. According with the literature, the stoichiometry of the CO adsorption on the metallic atoms was assumed to be 1 [45,46].

Transmission electron microscopy (TEM) images were obtained using two microscopes: a Jeol JEM 2100, operating with a LaB$_6$ filament at an accelerating voltage of 200 kV, with a point resolution of 0.25 nm, and a Jeol JEM 2011 instrument (LaB$_6$ filament, 200 kV, 0.18 nm point resolution). Each microscope was equipped with an XEDS unit (Oxford INCA) and a Gatan CCD camera. The samples were previously ground, suspended in ethanol and deposited onto holey carbon-coated Cu grids.

The X-ray diffraction (XRD) patterns were obtained in a X'Pert PRO Panalytical difractometer, using Cu Kα monochromatic radiation (0.154056 nm), a scanning range of 10–100° and a scan step size of 0.03 s^{-1} with 5 s collection time.

The surface composition of the catalysts was analyzed by X-ray photoelectron spectroscopy (XPS) (5700C Multitechnique System, Physical Electronics), using Mg–Kα (1253.6 eV) radiation. The ele-

diminishing the metal sintering and/or improving the thermal and chemical stability of the catalyst, thus playing an important role in the catalytic activity. Activated carbon (AC) is frequently used as catalyst support due to its thermal stability and mechanical resistance, its high porosity and specific surface, which confers it a high adsorption capacity, and its good chemical resistance (except at high temperatures under oxidant atmosphere), as well as its relatively low price [19–22].

In the last years, in order to improve their properties, an increasing number of catalysts whose active phases include more than one metal are being used for the sake of combining their respective abilities with better results in terms of behaviour and economy [23–27]. One of the main advantages observed in these bimetallic systems is an improved dispersion of the active phase [23,28,29]. Besides, the literature reports studies where bimetallic catalysts show higher activity than the homologous monometallics [30,31] although there is a lack in understanding the real structure and morphology of these bimetallic materials, and the nature of the synergistic effects observed are not always comprehensively explained since the characteristics of those bimetallic systems are still not completely understood [32].

In previous studies [16,17,33–36] the behaviour of four metallic phases (Pd, Pt, Rh and Ru) supported on activated carbon was analyzed in the gas-phase HDC of chloromethanes, finding significant differences in activity, selectivity and stability. Both the palladium and platinum catalysts (namely Pd/AC and Pt/AC) were highly selective to non-chlorinated products, especially Pd/AC. However, while Pd/AC showed a higher initial activity, it suffered an important deactivation upon time on stream [33,34], whereas Pt/AC did not show signs of deactivation upon 26 days on stream [17,33,34,37]. The aim of this work is to analyze the catalytic activity of Pd–Pt bimetallic catalysts supported on activated carbon in the HDC of DCM, in comparison with the behaviour shown by homologous monometallics. Even supported in materials different than activated carbon, this Pd–Pt combination has already been reported in the scientific literature for the hydrodechlorination of chlorinated compounds (CFC-12 [38–40], carbon tetrachloride [38] and 1,2-dichloroethane [38,41]), finding it a promising catalyst.

2. Experimental

2.1. Catalysts preparation

Two monometallic (Pd or Pt) and three bimetallic (Pd and Pt) catalysts supported on a commercial AC supplied by Merck (S_{BET}
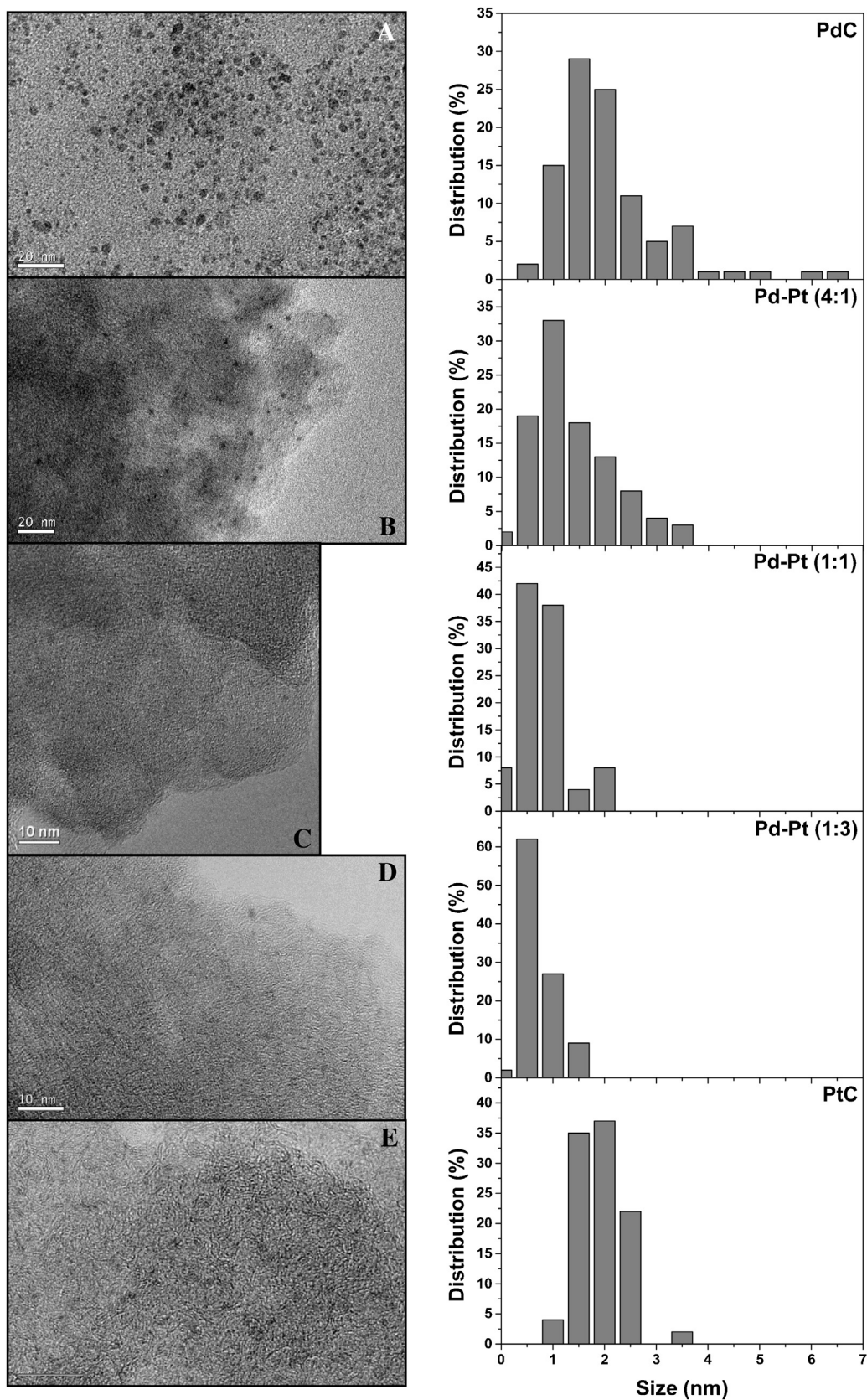
Fig. 2. HR-TEM images and size distribution of PdC (A), Pd–Pt (4:1) (B), Pd–Pt (1:1) (C), Pd–Pt (1:3) (D) and PtC (E).
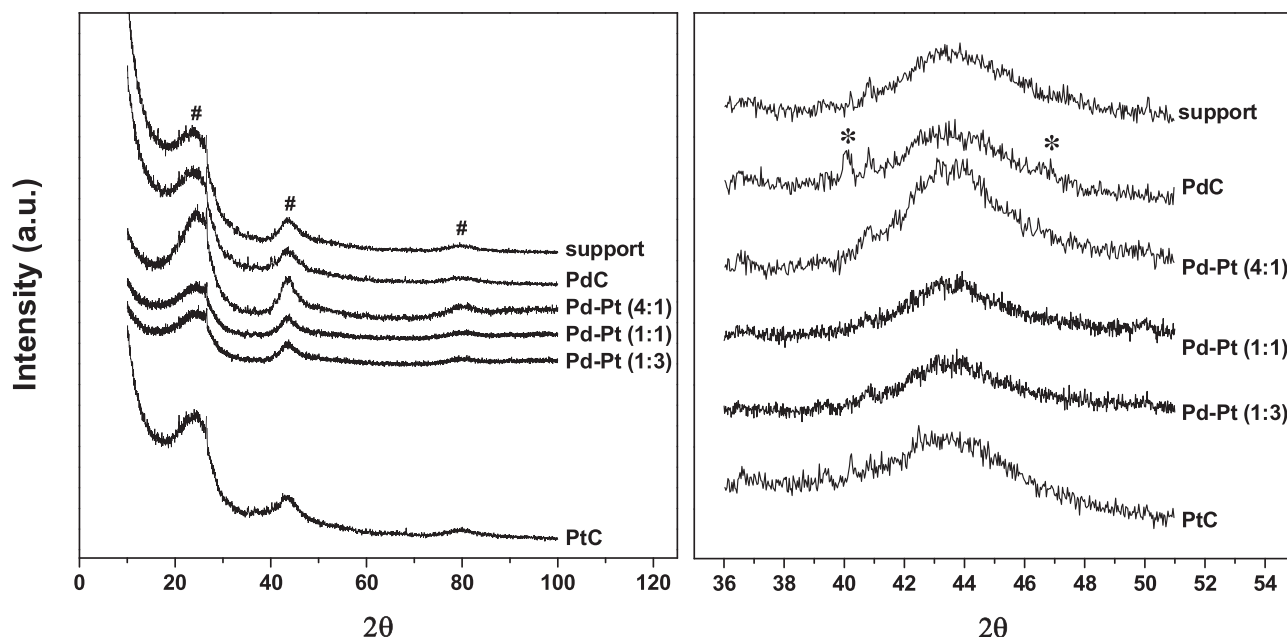
Fig. 3. XRD patterns of the catalysts and the carbon-support (left), and detail of 36–51° area (right).

ments present and its concentration were determined by recording general XPS spectra, scanning up to a binding energy (BE) of 1200 eV. The C 1s peak (284.6 eV) was taken as an internal standard to correct the shift in BE caused by sample charging. The BE of the Pd $3d_{5/2}$ and Pt $4f_{7/2}$ core levels and the full width at half maximum values were used to assess the chemical state of the metals on the catalyst surface, according to NIST database

2.3. Hydrodechlorination experiments

The HDC experiments were conducted in a continuous flow reaction system described elsewhere [47], consisting of a quartz fixed bed micro-reactor (8 mm i.d.) coupled to a gas-chromatograph with a flame ionization detector (FID) to analyze the reaction products.

The tests were performed at atmospheric pressure, a total gas flow rate of 100 Ncm^3 min^{-1}, a DCM inlet concentration of 1000 ppmv, a H$_2$/DCM molar ratio of 100 and a space-time (τ, ratio between the mass of catalyst used and the DCM molar flow) of 0.6 kg h mol^{-1}. Reaction temperatures of 150, 175 and 200 °C were tested. Besides, long term experiments (5 days under continuous operation) were performed at a reaction temperature of 200 °C.

The behaviour of the catalysts was evaluated in terms of DCM conversion, metallic intrinsic activity or turnover frequency (TOF), selectivity to the different reaction products, overall dechlorination and stability (evolution of the catalytic activity upon time on stream).

3. Results and discussion

3.1. Characterization of the catalysts

Table 2 summarizes the results of bulk metal content (by ICP-MS), porous structure (S_{BET} and V_{micro}), metal dispersion and metallic particle size (by TEM) of the catalysts prepared. The ICP-MS analysis confirm that the measured Pd and Pt contents lie close to the nominal values calculated from the amounts of the precursors used in each case. The 77 K N$_2$ adsorption–desorption isotherms (not shown) approach Type 1 of the DBBT classification [48,49], characteristic of microporous solids, as corresponds to the acti-

vated carbon support, whose BET surface area an micropore volume are only slightly higher than those of the catalysts. Therefore, the introduction of the metallic phase does not affect significantly the porous structure of the catalysts.

Fig. 1 shows the TPR profiles of the catalysts. All of them exhibit only one peak associated with the reduction of the metallic species. In the monometallic PdC catalyst this peak can be attributed to the reduction of Pd^{2+} to Pd^0 at 227 °C. This temperature is higher than that found by other authors in catalysts prepared from the same Pd precursor supported in different materials, indicating that the interaction of PdCl$_2$ with activated carbon is stronger than with other supports, e.g. SiO$_2$, Al$_2$O$_3$, La$_2$O$_3$, ZrO$_2$ or CeO$_2$ [50–55]. For palladium catalysts prepared with an AC-Erkimia as support, peaks at 240 °C [14] and 233 °C [35] were obtained. In the monometallic Pt catalyst (PtC) the peak associated to Pt^{2+} reduction appears at 231 °C, close to the 240 °C [14] and 244 °C [35] on AC-Erkimia. In the bimetallic catalysts appears only one reduction peak around 220 °C. This lower temperature of the reduction of the bimetallic catalysts compared to the monometallic ones suggests that the metallic particles might be smaller in the former and thus easier to reduce, which is consistent with the higher dispersion values of the bimetallic samples obtained by CO chemisorption and supported by the TEM images that will be analyzed below. There is a small peak showing H$_2$ consumption at high temperature (>600 °C) in all the TPR profiles. According to the observations of other authors it can be attributed to the gasification of the carbon support-catalyzed by the metals, or to the interaction of H$_2$ with the active sites created on the carbon surface upon decomposition of oxygen functional groups during TPR [56,57].

The results of CO chemisorption (Table 2) indicate that the metal phase is fairly well dispersed in all the catalysts, although better in the bimetallic ones. It seems that the addition of small amounts of Pt has a major effect on dispersion. Different authors have observed this improved dispersion in bimetallic respect to the monometallic homologous [23,28,29].

The increase of dispersion in the bimetallic catalysts is associated to lower metal particles size. Fig. 2 shows high resolution TEM micrographs and size distributions of the metallic particles of the catalysts. In all cases, fairly narrow distributions were obtained with smaller mean diameters for the bimetallic catalysts, some of
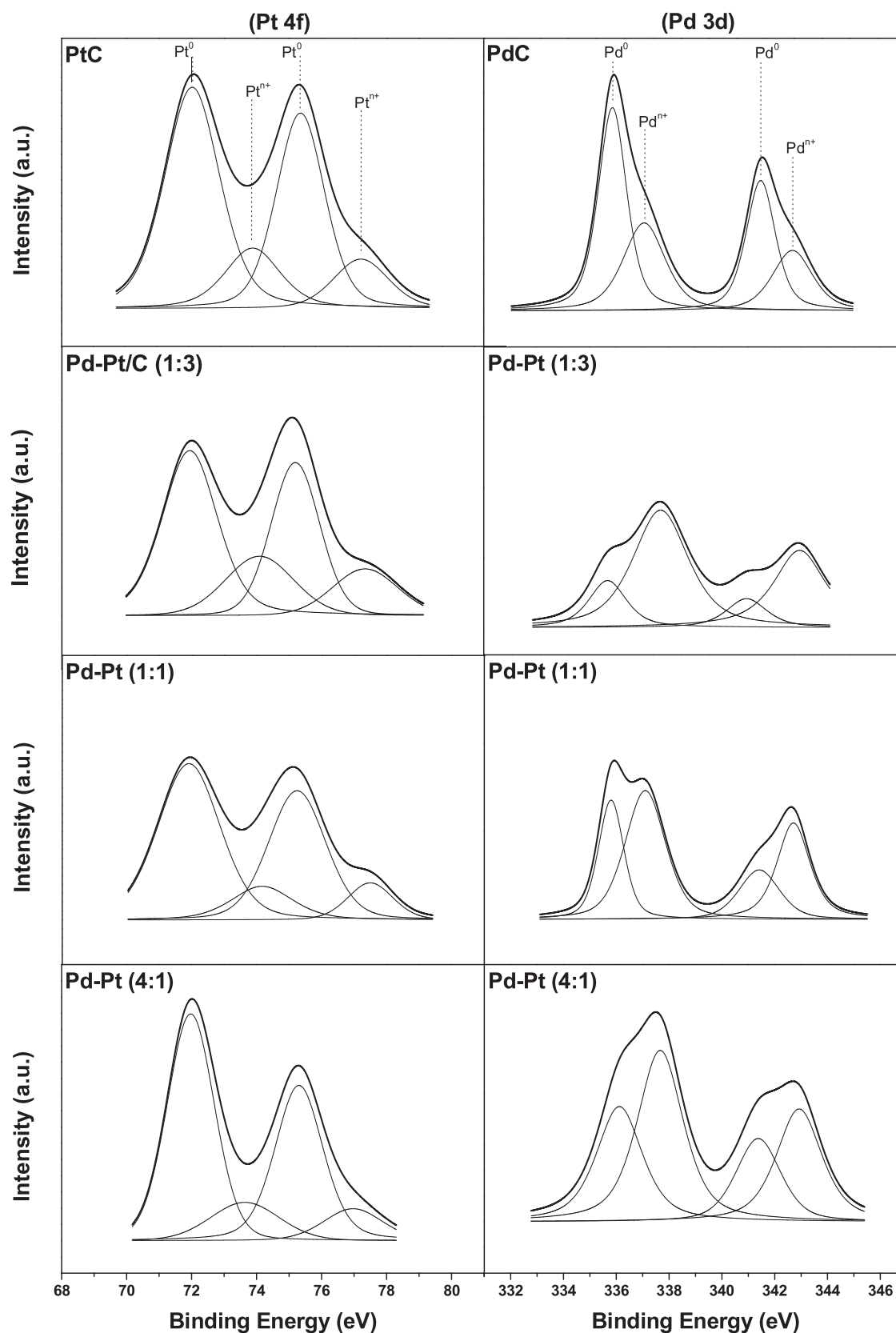
Fig. 4. XPS profiles in the Pt 4f region (left) and the Pd 3d region (right) of the catalysts.

them showing even metallic particles of sub-nanometric dimensions. The mean diameter values calculated from TEM images are collected in Table 2.

The XRD patterns of the catalysts are shown in Fig. 3 which includes that of the carbon support for comparison. All the diffractograms show the main peaks of the carbon support (#) around
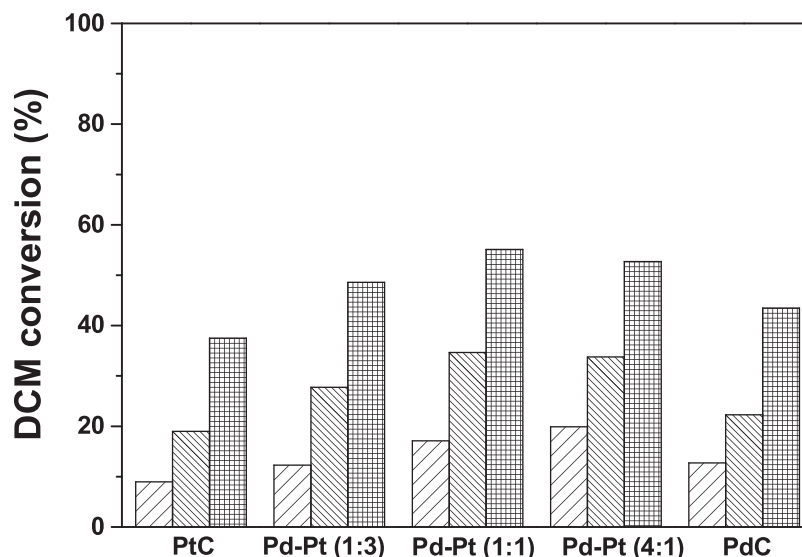
Fig. 5. DCM conversion obtained with each catalyst at different reaction temperatures: 150 °C (⬚), 175 °C (⬚), 200 °C (⬚).

Table 2

Metal content (ICP-MS), porous structure (S_{BET} and V_{micro}), metal dispersion (by CO chemisorption) and metal particle size (mean from TEM) of the catalysts.

Catalyst	Metal content (wt.%)		S_{BET} (m^2 g^{-1})	V_{micro} (cm^3 g^{-1})	Dispersion (%)	Metal size (nm)
	Pd	Pt				
PtC	–	1.73	724	0.31	17	1.7
Pd–Pt (1:3)	0.24	1.27	723	0.29	25	0.6
Pd–Pt (1:1)	0.45	0.85	737	0.30	32	0.7
Pd–Pt (4:1)	0.86	0.32	719	0.28	36	1.1
PdC	0.91	–	716	0.29	24	1.8

26° (0 0 2 planes), 43° (1 0 0, 1 0 1 and 1 0 2 planes, indistinguishable) and 80° (1 1 0 planes) [58–60]. The main peaks associated to Pd and Pt should appear at 40.1° and 39.8°, respectively (1 1 1 planes) [35,61]. This region of the spectra is depicted in detail in the right part of the Fig. 3. As can be seen, only the monometallic Pd catalyst shows a peak due to the metal. A second peak associated to (2 0 0) planes can also be observed in this catalyst at 46.7° (*). The presence of those diffraction peaks suggests the existence of a certain amount of larger Pd particles in that catalyst, consistent with the wider size distribution obtained by TEM. The same was observed in previous studies of Pd catalysts supported in activated carbon [16,33–35]. The fact that peaks associated with the metals in the Pt-containing catalysts were not found is consistent with the TPR, TEM and dispersion results since the metallic particles in those catalysts are smaller and better dispersed on the support.

The XPS spectra (Fig. 4) show the existence of two different metallic species in the catalysts, zero-valent (M^0)—originated upon reduction of the precursor, and electro-deficient (M^{n+})—whose relative occurrence depends on the nature of the support and the precursor as well as on the method for catalyst preparation [62–66]. The existence of these dual active sites has been described before in carbon-supported metallic catalysts used in the HDC of DCM [16,33,47,67]. Furthermore, in recent studies [34,68] the density functional theory was applied to the gas-phase HDC of DCM with palladium and platinum catalysts, finding that both, dissociative and non-dissociative adsorption of DCM on the Pd/Pt surface, imply high adsorption enthalpies, being, however, the non-dissociative adsorption of DCM over the electro-deficient species remarkably favored in terms of energy for both metals.

The Pt 4f region of the XPS spectra (left) shows the existence of a doublet in all the cases, corresponding to Pt 4f$_{5/2}$ and Pt 4f$_{7/2}$, and separated 3.33 eV due to spin orbital splitting. A similar analysis of the Pd 3d region show a doublet corresponding to Pd 3d$_{3/2}$ and

Table 3

Bulk (ICP) to surface (XPS) metal ratios and relative distribution of zero-valent and electro-deficient species on the surface of the catalysts (atomic composition).

Catalyst	Pd$_{XPS/ICP}$	Pt$_{XPS/ICP}$	Pd^0 (%)	Pd^{n+} (%)	Pt^0 (%)	Pt^{n+} (%)
PtC	–	0.7	–	–	78.0	22.0
Pd–Pt (1:3)	1.5	0.6	21.2	78.8	81.4	18.6
Pd–Pt (1:1)	1.6	1.3	30.7	69.3	82.0	18.0
Pd–Pt (4:1)	1.1	1.5	44.9	55.1	86.0	14.0
PdC	11.3	–	57.3	42.7	–	–

Pd 3d$_{5/2}$, separated 5.26 eV [69]. The deconvolution of the spectra shows the existence of two different species in each case. The peaks lying around 72.0 eV and 75.3 eV can be attributed to Pt^0, while the peaks around 73.8 eV and 77.2 eV correspond to Pt^{n+}. Similarly, the peaks around 335.5 eV and 340.8 eV are related with Pd^0, and the ones around 336.7 eV and 342.0 eV correspond to Pd^{n+}. These values of binding energy (BE) are similar to those found previously in mono and bimetallic palladium and platinum catalysts prepared with the same metal precursor [17,33–35,54]. The relative distribution of metal species on the catalysts surface, measured by XPS, is summarized in Table 3. In the case of platinum, it can be seen that Pt^0 is by far the prevailing specie in all the cases, in agreement with previous studies with Pt on AC catalysts [17,33–35]. The opposite occurs with palladium, where, except for the monometallic catalysts, the electro-deficient species predominates although a more balanced situation than for platinum is observed. Pt has a somewhat higher reduction potential than Pd although it seems unlikely that such markedly different distribution of species can be so explained by that reason. As can be seen, the proportion of zero-valent species of both Pd and Pt increases with the relative amount of Pd in the catalyst. Looking at the XPS to ICP metal ratios of Table 3, in general the metallic phase of the bimetallic catalysts is quite homogeneously distributed throughout the support although
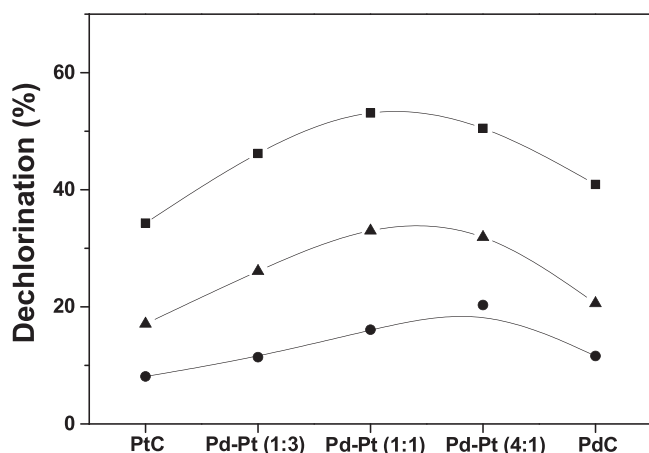
Fig. 6. Global dechlorination obtained with each catalyst in the HDC of DCM at different reaction temperatures: 150 °C (●), 175 °C (▲), 200 °C (■).
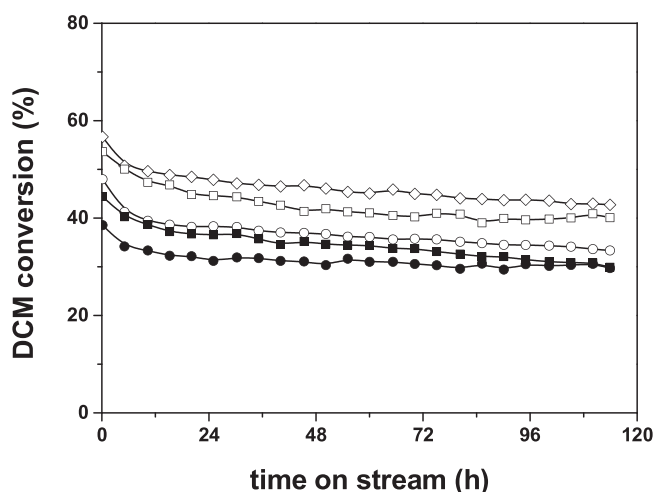

Fig. 7. Evolution of DCM conversion upon time on stream in long-term experiments with the catalysts tested ($T = 200$ °C): PtC (●), PdC (■), Pd–Pt (1:3) (○), Pd–Pt (1:1) (◇), Pd–Pt (4:1) (□).

Table 4
Selectivity to reaction products from the experiments of Fig. 5.

Catalyst	Temperature(°C)	Selectivity (%)		
		CH_4	C_2H_6	MCM
PtC	150	79.2	–	20.8
	175	80.3	–	19.7
	200	83.2	–	16.8
Pd–Pt (1:3)	150	85.8	–	14.2
	175	87.9	–	12.1
	200	90.2	–	9.8
Pd–Pt (1:1)	150	88.2	–	11.8
	175	90.5	–	9.6
	200	92.2	0.6	7.2
Pd–Pt (4:1)	150	83.2	2.4	14.4
	175	85.4	3.2	11.5
	200	86.7	5.0	8.4
PdC	150	80.7	1.6	17.7
	175	80.7	4.5	14.8
	200	80.2	8.0	11.9

Table 5
Initial TOF values calculated for the catalysts tested.

Catalyst	TOF (h^{-1})	
	150 °C	175 °C
PtC	56.94	120.68
Pd–Pt (1:3)	53.11	119.96
Pd–Pt (1:1)	57.73	117.05
Pd–Pt (4:1)	58.69	101.37
PdC	57.35	100.29

somewhat more concentrated in the outer surface (except for Pt in Pd:Pt 1:3). The monometallic catalysts show dramatic differences in that respect since opposite to the more or less homogeneous distribution of Pt with somewhat higher concentration towards the internal surface, the Pd catalyst shows a frankly defined egg-shell distribution with the metallic phase in the outermost surface. The wider metal particle size distribution of this last can favor a higher concentration towards the external part of the AC support but it seems insufficient to explain the dramatic differences between the two monometallic catalysts.

3.2. Catalytic activity

Fig. 5 shows the DCM conversion achieved with the catalysts tested at 0.6 kg h mol^{-1} space-time and different temperatures within the 150–250 °C range. The overall dechlorination is depicted in Fig. 6, and Table 4 summarizes the selectivities to reaction products. The bimetallic catalysts yielded always better results than the monometallic ones indicating a synergistic effect between both metals. Among the bimetallic catalysts tested the one with equimolar Pd/Pt ratio yielded the best results. According to previous results [17,33,35] obtained in the HDC of chloromethanes with activated carbon-supported Pd and Pt catalysts, the activity of the Pd ones increased with the proportion of electro-deficient species (Pd^{n+})

while the opposite was observed for Pt-based catalysts, where increasing the proportion of zero-valent species (Pt^0) enhanced the activity. Now, it can be seen that in the three bimetallic catalysts Pt is mostly as Pt^0 and Pd as Pd^{n+}. Moreover, above all, the bimetallic catalysts present the highest metal dispersions, especially Pd–Pt (1:1) and Pd–Pt (4:1) (Table 2), and the smaller particles size (Fig. 2), consistently with the higher DCM conversion and overall dechlorination achieved.

In order to establish the metallic contribution to the catalyst activity, Table 5 compares the TOF values of each catalyst at 150 °C and 175 °C. No significant differences in the metal contribution to the activity are observed, what reinforces the idea of the higher activity being caused by the smaller metal particles in the bimetallic catalysts. However, a slight decrease of TOF is observed at 175 °C for the catalysts with the highest Pd content which could be related to the lower amount of Pd^{n+} in these catalysts, what explains the lower activity of Pd–Pt (4:1) when compared to Pd–Pt (1:1) despite its higher dispersion. In previous works, density functional theory (DFT) analysis were conducted for the HDC of DCM with Pd and Pt catalysts to achieve a better knowledge of the reaction mechanism involved in the process, finding that electro-deficient Pd^{n+} species interacts more effectively with the hydrogen molecule, resulting in a more energetically stabilized dissociated H intermediates [34,68].

As expected, increasing the temperature increases the activity but it is important to remark that this effect is more significant in the case of the bimetallic catalyst, most in particular for the Pd–Pt (1:1) where a 5-fold increase of the overall dechlorination was achieved along the 50 °C difference of the range tested. Methane was always by far the main reaction product and it was accompanied only by MCM except for the catalysts with a higher Pd content, namely the monometallic Pd catalyst and the bimetallic Pd–Pt (4:1) one. Those catalysts have a higher Pd^{n+}/Pd^0 ratio which has been found in a previous work to favour the formation

of hydrocarbon species heavier than methane upon dechlorination of chloromethanes [33].

These experiments were carried out in mild conditions in order to determine the TOF values and compare the catalysts activity. An additional experiment at higher temperature (250 °C) and space-time (1.73 kg h mol^{-1}) was done with Pd–Pt (1:1), obtaining a DCM conversion of 100% and a global dechlorination of 98.6%, proving the good behaviour of this material to operate as hydrodechlorination catalysts.

Regarding the catalyst stability, Fig. 7 shows the evolution of DCM conversion upon time on stream at 200 °C and 0.6 kg h mol^{-1} space-time with the catalysts tested. As can be seen, all of them suffer a loss of activity during the first 12 h under continuous operation at 200 °C. After, they show a fairly stable behaviour, being the Pt catalyst (PtC) the best one in that respect, with only 8% loss of activity within the following 100 h on stream. Under the same conditions, PdC, on the contrary, suffers a loss of activity of about 20%. In general, it seems that the presence of Pt improves somewhat the stability of the bimetallic catalysts whereas Pd contributes to increase DCM conversion.

4. Conclusions

The use of bimetallic catalysts of Pd and Pt in the gas-phase HDC of DCM results in a synergistic effect respect the catalytic activity when compared to the monometallic ones, that can be ascribed to a significant increase in metal dispersion, leading to metallic particles of sub-nanometre size (1.1, 0.7 and 0.6 nm for Pd–Pt (4:1), Pd–Pt (1:1) and Pd–Pt (1:3), respectively). These bimetallic systems transform DCM to non-chlorinated products more efficiently than the analogous monometallic Pd and Pt catalysts, substantially improving their DCM conversion and global dechlorination. With regard to the stability, it has been proved that the presence of Pt improves the catalysts life, enhancing the PdC stability. Among the catalysts tested, the higher activity and global dechlorination were obtained with the catalyst with the same molar-contain of both metals (Pd–Pt (1:1)) what can be attributed to its high metal dispersion (and small particle size) and its optimum ratio of Pd^{n+} and Pt^0 species.

Acknowledgements

References

[1] W.J. Hayes Jr., E.R. Laws Jr., Handbook of pesticide toxicology General Principles, vol. 1, Academic Press, San Diego, 1991.
[2] US EPA, in: Pollution prevention research, Needs for eleven TRI organic chemical groups, Washington DC, 1991.
[3] P. Ciccioli, Chemistry and Analysis of Volatile Organic Compounds in the Environment, in: H.J.T. Bloemen, J. Burn (Eds.), Springer Netherlands, Glasgow, 1993, pp. 92–174.
[4] E. Dobrzynska, M. Posniak, M. Szewczynska, B. Buszewski, Crit. Rev. Anal. Chem. 40 (2010) 41–57.
[5] ECSA, Ing. Quim. 307 (1994) 101–109.
[6] C.J. Noelke, H.F. Rase, Ind. Eng. Chem. Prod. Res. Dev. 18 (1979) 325–328.
[7] S. Ordonez, H. Sastre, F.V. Diez, Recent Res. Dev. Chem. Eng. 4 (2000) 327–339.
[8] F.J. Urbano, J.M. Marinas, J. Mol. Catal. A: Chem. 173 (2001) 329–345.
[9] L.M. Gómez-Sainero, M. Martin-Martinez, M.A. Alvarez-Montero, J. Bedia, A. Arevalo-Bastante, J.J. Rodriguez, CHISA 2014 (2014).
[10] R.M. Lago, M.L.H. Green, S.C. Tsang, M. Odlyha, Appl. Catal. B 8 (1996) 107–121.
[11] R. Bonny, C. Lenfant, F.C. Thyrion, Int. J. Environ. Stud. 53 (1/2) (1997) 75–85.
[12] R. Brukh, S. Mitra, R. Barat, Combust. Sci. Technol. 176 (2004) 531–555.
[13] L. Prati, M. Rossi, Appl. Catal. B 23 (1999) 135–142.
[14] L.M. Gomez-Sainero, A. Cortes, X.L. Seoane, A. Arcoya, Ind. Eng. Chem. Res. 39 (2000) 2849–2854.
[15] S. Ordonez, H. Sastre, F.V. Diez, Appl. Catal. B 25 (2000) 49–58.
[16] M.A. Alvarez-Montero, L.M. Gomez-Sainero, M. Martin-Martinez, F. Heras, J.J. Rodriguez, Appl. Catal. B 96 (2010) 148–156.
[17] M.A. Alvarez-Montero, L.M. Gomez-Sainero, A. Mayoral, I. Diaz, R.T. Baker, J.J. Rodriguez, J. Catal. 279 (2011) 389–396.
[18] M.A. Keane, ChemCatChem. 3 (2011) 800–821.
[19] J. Blanco, R. Linarte, Catálisis: Fundamentos y Aplicaciones Industriales, first ed., Trillas, México, 1976.
[20] H. Juentgen, Fuel 65 (1986) 1436–1446.
[21] R.C. Bansal, F. Stoeckli, J. Donnet, Active Carbon, CRC Press, New York, 1988.
[22] C. Amorim, M.A. Keane, J. Chem. Technol. Biotechnol 83 (2008) 662–672.
[23] Y.C. Cao, Y. Li, Appl. Catal. A 294 (2005) 298–305.
[24] J.W. Bae, E.J. Jang, B.I. Lee, J.S. Lee, K.H. Lee, Ind. Eng. Chem. Res. 46 (2007) 1721–1730.
[25] M. Lu, J. Sun, D. Zhang, M. Li, J. Zhu, Y. Shan, React. Kinet. Mech. Catal. 100 (2010) 99–103.
[26] Z. Karpinski, M. Bonarowska, W. Juszczyk, Pol. J. Chem. Technol. 16 (2014) 101–105.
[27] M. Bonarowska, Z. Kaszkur, D. Lomot, M. Rawski, Z. Karpinski, Appl. Catal. B 162 (2015) 45–56.
[28] G. Yuan, C. Louis, L. Delannoy, M.A. Keane, J. Catal. 247 (2007) 256–268.
[29] M. Legawiec-Jarzyna, W. Juszczyk, M. Bonarowska, Z. Kaszkur, L. Kepinski, Z. Kowalczyk, Z. Karpinski, Top. Catal. 52 (2009) 1037–1043.
[30] C.B. Molina, A.H. Pizarro, J.A. Casas, J.J. Rodriguez, Water Sci. Technol. 65 (2012) 653–660.
[31] J.A. Baeza, L. Calvo, J.J. Rodriguez, E. Carbo-Argibay, J. Rivas, M.A. Gilarranz, Appl. Catal. B 168 (2015) 283–292.
[32] A. Villa, D. Wang, D.S. Su, L. Prati, Catal. Sci. Technol. 5 (2015) 55–68.
[33] M. Martin-Martinez, L.M. Gomez-Sainero, M.A. Alvarez-Montero, J. Bedia, J.J. Rodriguez, Appl. Catal. B. 132 (2013) 256–265.
[34] M. Martin-Martinez, A. Alvarez-Montero, L.M. Gomez-Sainero, R.T. Baker, J. Palomar, S. Omar, S. Eser, J.J. Rodriguez, Appl. Catal. B 162 (2015) 532–543.
[35] M.A. Alvarez-Montero, L.M. Gomez-Sainero, J. Juan-Juan, A. Linares-Solano, J.J. LRodriguez, Chem. Eng. J. 162 (2010) 599–608.
[36] M.A. Álvarez-Montero, M. Martin-Martinez, L.M. Gómez-Sainero, A. Arevalo-Bastante, J. Bedia, J.J. Rodriguez, Ind. Eng. Chem. Res. 54 (7) (2015) 2023–2029.
[37] L.M. Gómez Sainero, J.J. Rodríguez Jiménez, A. Álvarez Montero, M. Martín Martínez, ES Patent, 2, 351130, 2011.
[38] M. Legawiec-Jarzyna, A. Srebowata, W. Juszczyk, Z. Karpinski, Appl. Catal. A 271 (2004) 61–68.
[39] M. Legawiec-Jarzyna, A. Srebowata, W. Juszczyk, Z. Karpinski, Catal. Today 88 (2004) 93–101.
[40] M. Bonarowska, Z. Karpinski, Catal. Today 137 (2008) 498–503.
[41] M.C. García, L.G. Woolfolj, N. Martín, A. Granados, J.A. de los Reyes, Rev. Mex. Ing. Chim. 11 (2012) 463–468.
[42] S. Brunauer, P.H. Emmett, E. Teller, J. Am. Chem. Soc. 60 (1938) 309–319.
[43] G. Halsey, J. Chem. Phys. 16 (1948) 931–937.
[44] B.C. Lippens, B.G. Linsen, J.H. de Boer, J. Catal. 3 (1964) 32–37.
[45] S.H. Ali, J.G. Goodwin Jr., J. Catal. 176 (1998) 3–13.
[46] N. Mahata, V. Vishwanathan, Catal. Today 49 (1999) 65–69.
[47] Z.M. de Pedro, L.M. Gomez-Sainero, E. Gonzalez-Serrano, J.J. Rodriguez, Ind. Eng. Chem. Res. 45 (2006) 7760–7766.
[48] S. Brunauer, L.S. Deming, W.E. Deming, E. Teller, J. Am. Chem. Soc. 62 (1940) 1723–1732.
[49] J. Haber, Pure Appl. Chem. 63 (1991) 1227–1246.
[50] J.S. Rieck, A.T. Bell, J. Catal. 96 (1985) 88–105.
[51] R. Ohnishi, W.L. Wang, M. Ichikawa, Appl. Catal. A 113 (1994) 29–41.
[52] N.S. Figoli, P.C. Largentiere, A. Arcoya, X.L. Seoane, J. Catal. 155 (1995) 95–105.
[53] L.M. Gomez-Sainero, R.T. Baker, I.S. Metcalfe, M. Sahibzada, P. Concepcion, J.M. Lopez-Nieto, Appl. Catal. A 294 (2005) 177–187.
[54] J. Bedia, L.M. Gomez-Sainero, J.M. Grau, M. Busto, M. Martin-Martinez, J.J. Rodriguez, J. Catal. 294 (2012) 207–215.
[55] S. Lin, L. Yang, X. Yang, R. Zhou, Appl. Surf. Sci. 305 (2014) 642–649.
[56] S.R. de Miguel, J.I. Villella, E.L. Jablonski, O.A. Scelza, C.S.M. de Lecea, A. Linares-Solano, Appl. Catal. A 232 (2002) 237–246.
[57] I.M. Vilella, S.R. de Miguel, O.A. Scelza, Chem. Eng. J. 114 (2005) 33–38.
[58] A.D. Lueking, H.R. Gutierrez, P. Jain, D.T. Van Essandelft, C.E. Burgess-Clifford, Carbon 45 (2007) 2297–2306.
[59] A. Nieto-Marquez, J.L. Valverde, M.A. Keane, Appl. Catal. A 332 (2007) 237–246.
[60] J. Zhao, L. Yang, F. Li, R. Yu, C. Jin, Carbon 47 (2009) 744–751.
[61] K. Persson, A. Ersson, S. Colussi, A. Trovarelli, S.G. Jaras, Appl. Catal. B 66 (2006) 175–185.
[62] P.A. Simorov, E.M. Moroz, A.L. Chuvilin, V.N. Kolomiichuk, A.I. Boronin, V.A. Likholobov, Stud. Surf. Sci. Catal. 91 (1995) 977–987.
[63] S. Jujjuri, E. Ding, E.L. Hommel, S.G. Shore, M.A. Keane, J. Catal. 239 (2006) 486–500.
[64] E. Ding, S. Jujjuri, M. Sturgeon, S.G. Shore, M.A. Keane, J. Mol. Catal. A: Chem. 294 (2006) 51–60.
[65] M.I. Cobo, J.A. Conesa, C.M. de Correa, J. Phys. Chem. A 112 (2008) 8715–8722.
[66] N.S. Babu, N. Lingaiah, N. Pasha, J.V. Kumar, P.S.S. Prasad, Catal. Today 141 (2009) 120–124.

[67] L.M. Gomez-Sainero, X.L. Seoane, J.L.G. Fierro, A. Arcoya, J. Catal. 209 (2002) 279–288.

[68] S. Omar, J. Palomar, L.M. Gomez-Sainero, M.A. Alvarez-Montero, M. Martin-Martinez, J.J. Rodriguez, J. Phys. Chem. C 115 (2011) 14180–14192.

[69] J.F. Moulder, W.F. Stickle, P.E. Sobol, K.D. Bomben, Handbook of X-ray photoelectron spectroscopy: A reference book of standard data for use in X-ray photoelectron spectroscopy, in: Physical Electronics Division, PerkinElmer Corp, 2015.